Journal of Pharmaceutical and Biomedical Analysis 200 (2021) 114073

Contents lists available at ScienceDirect

Journal of Pharmaceutical and Biomedical Analysis

journal homepage: www.elsevier.com/locate/jpba

Investigation of the therapeutic effect of Yinchen Wuling Powder on CCl_4-induced hepatic fibrosis in rats by ^1H NMR and MS-based metabolomics analysis

Yumeng Zhang [a,1], Min Zhao [a,1], Yangyang Liu [b], Tingting Liu [a], Chunjie Zhao [a,*], Miao Wang [b,**]

[a] School of Pharmacy, Shenyang Pharmaceutical University, Wenhua Road 103, Shenyang, Liaoning, China
[b] School of Life Science and Biopharmaceutics, Shenyang Pharmaceutical University, Wenhua Road 103, Shenyang, Liaoning, China

ARTICLE INFO

Article history:
Received 6 February 2021
Received in revised form 27 March 2021
Accepted 10 April 2021
Available online 17 April 2021

Keywords:
Yinchen Wuling Powder
Hepatic fibrosis
Metabolomics
^1H NMR
UPLC-MS

ABSTRACT

Hepatic fibrosis (HF) is a typical consequence of various chronic liver diseases, and there is still no ideal drug for its treatment. Yinchen Wuling Powder (YCWLP), a famous traditional Chinese medicine prescription, is effective for the treatment of icteric hepatitis, hepatic fibrosis, non-alcoholic fatty liver disease and other liver diseases in clinical practices, however, the underlying mechanisms of YCWLP on HF is still unclear. In this study, ^1H NMR and MS-based metabolomics analysis along with body weight change, serum liver function indexes, serum liver fibrosis index and histopathological observations of liver were applied to evaluate the therapeutic effect of YCWLP on hepatic fibrosis and the mechanism associated with this. The results of the pharmacodynamics study show that YCWLP has a significant therapeutic effect on hepatic fibrosis. As for the metabolomics research, 7 metabolites in the plasma samples, 28 in the urine samples and 6 in the liver samples were significantly altered due to the protective effect of YCWLP on CCl_4-induced hepatic fibrosis. These endogenous metabolites are involved in amino acid metabolism, carbohydrate metabolism, glycerophospholipid metabolism and gut bacteria metabolism. These findings suggest that YCWLP could treat hepatic fibrosis by promoting urea circulation and reducing blood ammonia accumulation, improving carbohydrate metabolism and reducing oxidative stress, improving glycerophospholipid metabolism and protecting cell membrane, and regulating intestinal flora metabolism.

1. Introduction

Hepatic fibrosis is the result of the damage-repair reaction of the liver caused by various pathogenic factors. Its main pathological change is the excessive deposition of extracellular matrix (ECM) in the liver. If not treated in time, it will progress to decompensated cirrhosis and arise a variety of end-stage liver complications, which seriously affect the health of patients and even threaten their lives. Therefore, the treatment of hepatic fibrosis is particularly important. Since the 1990s, the progress of pathological research suggests that hepatic fibrosis is reversible [1]. It is possible to delay and reverse hepatic fibrosis, even early cirrhosis, if timely treatment is taken according to the etiology or inhibiting the synthesis and promoting the degradation of ECM in the liver. Although the modern pharmacological research of anti-hepatic fibrosis has been carried out for many years, there is still no ideal drug for the treatment of hepatic fibrosis.

Traditional Chinese medicine (TCM) has been used to treat liver diseases for thousands of years. Many years of clinical trials have proved that Chinese herbal medicine, especially TCM prescription, has a good anti-hepatic fibrosis effect, and has less toxic and side effects. Yinchen Wuling powder (YCWLP) is a famous TCM prescription with a long history. According to *Synopsis of the Golden Chamber* written by Zhang Zhongjing, a famous physician in the Eastern Han Dynasty, YCWLP has the effect of removing jaundice and eliminating dampness and composed of 6 herbal materials, including *Artemisia Capillaris Herba*, *Polyporus Umbellatus*, *Alismatis Rhizoma*,

* Corresponding author at: School of Pharmacy, Shenyang Pharmaceutical University, No. 103 Wenhua Road, Shenyang, 110016, Liaoning, China.
** Corresponding author at: School of Life Science and Biopharmaceutics, Shenyang Pharmaceutical University, No. 103 Wenhua Road, Shenyang, 110016, Liaoning, China.
E-mail addresses: lab433@163.com (C. Zhao), wangmiao_77111@hotmail.com (M. Wang).
[1] These authors contributed equally.

https://doi.org/10.1016/j.jpba.2021.114073
0731-7085/

Atractylodes Macrocephalae Rhizoma stir-fried with wheat bran, *Poria* and *Cinnamomi Ramulus* [2]. Clinically, it is mainly used in the treatment of neonatal jaundice [3], icteric hepatitis [4], liver ascites [5], hepatic fibrosis [6], non-alcoholic fatty liver disease [7] and other diseases. Modern pharmacological experiments and clinical trials have also confirmed the hepatoprotective effect of YCWLP [8,9], but its hepatoprotective mechanism is still unclear.

Metabolomics is a method for analyzing the dynamic and multi-channel metabolic response of organisms or cells under a specific physiological period. It involves the use of advanced high-throughput analytical chemistry techniques to characterize small molecular metabolites (molecular weight 100–1000) in biological fluids or tissues [10]. TCM is a complex system composed of multiple components, which can interfere with multiple targets of the body's metabolic network at the overall level [11]. Therefore, the systematic and holistic characteristics of metabolomics are suitable for the analysis of metabolic changes in the process of TCM intervention, and help to clarify its therapeutic mechanism. At present, nuclear magnetic resonance (NMR) and liquid chromatography-mass spectrometry (LC–MS) are common analytical techniques in metabolomics study. LC–MS is widely used in the study of unknown components in complex metabolomics samples due to its high sensitivity and strong separation ability [12]. However, MS has the following disadvantages: it can only detect ionizable compounds, has a matrix effect, and lacks robustness and repeatability. NMR is widely used in metabolomics because of its robustness, non-invasive, non-biased and short analysis time [13]. However, NMR method also has some shortcomings, such as low sensitivity and limited dynamic range. Therefore, in order to make up for the deficiencies, the combination of NMR and MS has become the most powerful tool in metabolomics analysis [14,15].

In this study, we used ^{1}H NMR and MS-based metabolomics combined with multivariate data analysis to explore the protective mechanism of YCWLP on CCl_4-induced hepatic fibrosis in rats. Moreover, potential biomarkers were screened in plasma, urine and liver samples for disease diagnosis and treatment evaluation. This study aims to assess the rationale of YCWLP in treating hepatic fibrosis and enhance its clinical use.

2. Material and methods

2.1. Drugs and chemicals

Artemisia Capillaris Herba (batch number: 190301), Polyporus Umbellatus (batch number: 1808079), Alismatis Rhizoma (batch number: 190705), Atractylodes Macrocephalae Rhizoma stir-fried with wheat bran (batch number: 1906091), Poria (batch number: 190601) and Cinnamomi Ramulus (batch number: 190401) were purchased from Shenyang Guoyaoda Pharmacy (Shenyang, China) and authenticated by Prof. Jia from Shenyang Pharmaceutical University (Shenyang, China). Silymarin (batch number: B1802965) was purchased from MADAUS GMBH (Cologne, Germany).

Sodium 3-trimethylsilyl-propionate [2,2,3,3,d_4] (TSP) and deuteroxide (D_2O) were purchased from Merck Drugs & Biotechnology (Germany). Heparin sodium was provided by National Pharmaceutical Group Rongsheng Pharmaceutical Co., Ltd (Henan, China). Acetonitrile (HPLC grade) and formic acid (LC/MS grade) were obtained from Fisher Inc. (Town, USA). Analytical grade disodium hydrogen phosphate, disodium hydrogen phosphate and formaldehyde were purchased from Kemeo Regent Co., Ltd (Tianjin, China). Purified water was purchased from Wahaha Co., Ltd. (Hangzhou, China). Hyaluronidase (HA), laminin (LN), type IV collagen (CIV), N-terminal propeptide of procollagen type III (PIIINP) assay ELISA kits were provided by Meimian Industrial Co., Ltd. (Jiangsu, China).

2.2. Preparation of YCWLP suspension

All crude drugs were ground into powder and then sieved through a 60 mesh stainless steel sieve. According to the records of *Synopsis of Golden Chamber*, YCWLP was prepared by mixing Artemisia Capillaris Herba, Polyporus Umbellatus, Alismatis Rhizoma, Atractylodes Macrocephalae Rhizoma stir-fried with wheat bran, Poria and Cinnamomi Ramulus at the weight ratio of 32:3:5:3:3:2 in powder form. The suspension (0.1 g/mL) was prepared by mixing YCWLP with normal saline, and used to feed rats in subsequent experiments. Before administration, the suspension was vortex mixed.

2.3. Animals and treatment

Male Sprague-Dawley rats (200 ± 20 g) were supplied by the Experimental Animal Center of Shenyang Pharmaceutical University (Liaoning, China). Animals were maintained in an environmentally controlled room under controlled temperature (20–25 °C) and relative humidity (40–70 %) with a 12 h light/dark cycle, and free access to standard diet and water. All rats were acclimated for 7 days prior to the experiment. All animal protocols in this study were approved by the Medical Ethics Committee of Shenyang Pharmaceutical University and in accordance with the guidelines of the National Institutes of Health on Animal Care (2004).

After acclimatization, twenty-four rats were randomly divided into four groups with six rats each: the control group (CON), the hepatic fibrosis group (HF), the YCWLP treatment group (YCWLP, 2 g/kg/d) and the positive group treated with silymarin (SYM, 50 mg/kg/d). The rats in the HF, YCWLP and SYM groups were orally administrated with 40 % (v/v) CCl_4 in soybean oil (2 mL/kg) twice a week for 13 weeks, while the CON group were administered with the same dose of soybean oil. Since the 6th week, the rats in the YCWLP group and SYM group were treated with YCWLP suspension (0.1 g/mL) and silymarin suspension (0.1 g/mL) respectively once daily for 8 weeks, while other rats were given the same dose of normal saline at the same time.

2.4. Sample collections

Urine (from 8:00 am to 8:00 am on the next day) and plasma samples were collected at the end of the 7th week, 9th week, 11th week, 13th week. Urine samples were collected using metabolism cages and transferred to a 4 °C refrigerator every 6 h, all urine of each rat was mixed evenly after collection. Plasma samples were obtained from the orbital venous plexus and transferred to Eppendorf tubes containing heparin sodium. All the urine and plasma samples were centrifuged at 1,100 g for 15 min and the supernatants were stored at -80 °C for metabolomics analysis.

At the end of the administration, all animals were anesthetized after an overnight fast. Then the rats were weighed and subjected to blood collection by puncturing the abdominal aorta. The serum samples were obtained by standing at 4 °C for 2 h and centrifuged at 1,100 g for 15 min, and the supernatants were collected for pharmacodynamic analysis. The liver of each rat was removed and divided into two parts. One part was immediately snap-frozen in liquid nitrogen and stored at -80°C for metabolomics analysis and the other part was fixed in 10 % formaldehyde for hematoxylin and eosin (H&E) staining.

2.5. Assessment of hepatic fibrosis

The body weight of each animal was monitored once a week. The liver tissues were fixed in 10 % formaldehyde for 24 h, embedded in paraffin and sectioned into 5 μm sections, then stained with hematoxylin-eosin. The morphological alterations of liver tissue

were assessed under a biological microscope by an independent researcher who was blinded to this study protocol.

Serum liver function index including alanine aminotransferase (ALT) and aspartate aminotransferase (AST) were carried out by the General Hospital of the northern theater of the Chinese people's Liberation Army. Serum liver fibrosis index including HA, LN, CIV and PIIINP were determined using the commercially available kits according to the manufacturers' instructions.

2.6. ^1H NMR metabolomics analysis

First, all samples were thawed at room temperature before analysis. 1.5 *g* liver sample of each rat was homogenized with 5 mL normal saline above the ice-water bath and centrifugated at 11,600 *g* for 10 min at 4 °C, then take the supernatant as the liver homogenate solution. Thereafter, 400 μL liver homogenate solution was mixed with 200 μL phosphate buffer (NaH_2PO_4-Na_2HPO_4, 0.2 M, pH 7.4) and centrifuged again at 11,600 *g* for 10 min at 4 °C. Finally, 450 μL supernatant was mixed with 100 μL TSP D_2O solution (1.0 mg/mL) and transferred to a 5 mm NMR tube for the metabolomics analysis. The preparation of plasma samples was the same as that of liver homogenate solution, except that the dosage of TSP D_2O solution was 200 μL. Regarding the urine samples, 500 μL of each sample was mixed with 100 μL phosphate buffer solution. Other treatments were the same as liver homogenate solution.

All NMR data were collected by Bruker AV 600 MHz superconducting Fourier transform NMR spectrometer (Bruker, Germany). At 298.2 K, plasma and liver samples were analyzed using Carr-Purcell-Meiboom-Gill spectra, urine samples were processed with a one-dimensional water presaturated standard NOESYPR 1D pulse sequence. Water peak was suppressed using a pre-saturation method. Deuterium (D_2O) + water (H_2O) was used for field frequency locking, and TSP was used as the chemical shift reference (1H, 0.00 ppm). ^1H NMR spectra were measured with 64 scans into 64 K data points over a spectral width of 12,019 Hz and a relaxation time of 2 s. An exponential function corresponding to a line broadening factor of 0.3 Hz was applied to all acquired free induction decays (FIDs) before Fourier transformation.

The data was analyzed using MestReNova 6.1.1 software (Mestrelab Research, USA). Each spectrum was manually phased and baseline corrected, the shape and chemical shift of TSP were used as the reference to adjust the phase and specify the zero point. The integral interval was δ 0 ~ 10.0 with an integral spacing of 0.04 ppm, the integral value of δ 4.7–5.2 was removed in order to eliminate the influence of the water peak, while the integral value of δ 5.6 ~ 6.2 was also removed in the urine to eliminate the influence of the urea peak. After normalization, the data were imported into SIMCA-P 13.0 (Umetrics, Umea, Sweden) for multivariate data analysis.

2.7. UPLC-MS metabolomics analysis

After thawing, 200 μL plasma sample of each rat was mixed with 600 μL pre-cooled acetonitrile, vortexing, and then centrifuged at 11,600 *g* for 10 min at 4 °C to obtain the supernatant. In the case of liver tissues, 100 μL liver homogenate solution was mixed with 600 μL pre-cooled acetonitrile, other treatments were the same as plasma sample. For the urine samples, 400 μL urine was diluted at a ratio of 1:1with pre-cooled water, vortexing, and then centrifuged at 11,600 *g* for 10 min at 4 °C. Finally, all the obtained supernatants were filtered with 0.22 μm microporous membrane filters for UPLC-MS analysis.

The UPLC-MS analysis was achieved by Waters ACQUITY UPLC system (Waters Corp., Milford, USA) equipped with a Universal XB C_{18} column (150 mm × 2.1 mm, 1.8 μm; Kromat, USA). The mobile phase comprised 0.1 % (v/v) formic acid-water (A) and 0.1 % (v/v) formic acid-acetonitrile (B), the flow rate was set at 0.2 mL/min and the elution procedures are shown in Table S1. The column temperature was 35 °C and the injected volume of each sample was 5 μL. MS analysis was performed by a Waters Quattro mass spectrometer coupled with a triple quadrupole mass analyzer (Waters Corp., Milford, MA, USA) in positive mode, and full scan mode was used with a range of 100−1000 Da. The parameters were set as followed: cone voltage, 35 V; capillary voltage, 3.2 kV; desolvation temperature, 350 °C; source temperature, 120 °C; desolvation flow rate, 600 L/h; cone gas flow rate, 50 L/h; collision energy, 10−30 eV.

Quality control (QC) samples were prepared by mixing equal volume of all plasma samples, urine samples and liver homogenate solutions, respectively. The repeatability was evaluated by injecting QC samples six times. During the whole analysis process, QC samples were analyzed every six specimens to measure the stability of the system. Six QC samples maintained at 4 °C for 24 h were analyzed to evaluate the post-preparative stability of the samples, and the freeze-thaw stability was assessed by analysis of six QC samples after three freeze-thaw cycles. The extracted ion chromatographic peaks of six ions were selected for method validation. The relative standard deviations (RSD) of the retention time (RT) and peak area were calculated and listed in Table S2. All values are less than 15 %, suggesting that the method is reliable.

The raw data were imported into Markerlynx V4.1 (Waters Corp., Milford, USA) for peak deconvolution and normalization. Then, a matrix of mass and retention time pairs with corresponding peak areas for all the detected peaks was obtained, and the matrix was imported into SIMCA-P 13.0 (Umetrics, Umea, Sweden) for multivariate data analysis.

2.8. Multivariate data analysis

All normalized data were imported into SIMCA-P 13.0 (Umetrics, Umea, Sweden), principal component analysis (PCA) and orthogonal projection to latent structure discrimination analysis (OPLS-DA) were performed to process the multivariate data analysis. The models were validated by the 7-fold cross-validation method and the permutation test (999 permutations). Plasma and urine samples at different time points were used for OPLS-DA metabolic trajectory analysis, to observe the time-dependent changes of YCWLP in the treatment of hepatic fibrosis. Loading plots were used to screen key metabolites between the CON and HF groups and between the HF and YCWLP groups, respectively. The key metabolites were selected according to the variable importance in projection (VIP) values (>1.2) from the OPLS-DA analysis and the p-values (<0.05) from the Student's t-test, and were identified by matching the chemical shift (^1H NMR) and the *m/z* (UPLC-MS) with the related literature [16–27] and available databases such as HMDB (http://www.hmdb.ca), MassBank (http://www.massbank.jp), METLIN (http://metlin.scripps.edu) and KEGG (http://www.genome.jp).

2.9. Screening for potential biomarkers and pathway analysis

The therapeutic effect of YCWLP is mainly reflected in its regulation of potential biomarkers of hepatic fibrosis. Thus, the metabolites with statistically significant changes both between the CON group and the HF group and between the HF group and the YCWLP group were regarded as key biomarkers regulated by YCWLP. Furthermore, SPSS 19.0 (Chicago, IL, USA) was used to perform receiver operating characteristic (ROC) curves, which were used to evaluate the predictive ability of metabolites. Metabolites with area under curve (AUC) > 0.85 were considered as potential biomarkers with excellent performance.

Finally, the potential biomarkers were imported into MetaboAnalyst 5.0 (http://metpa.metabolomics.ca) to analyze the metabolic

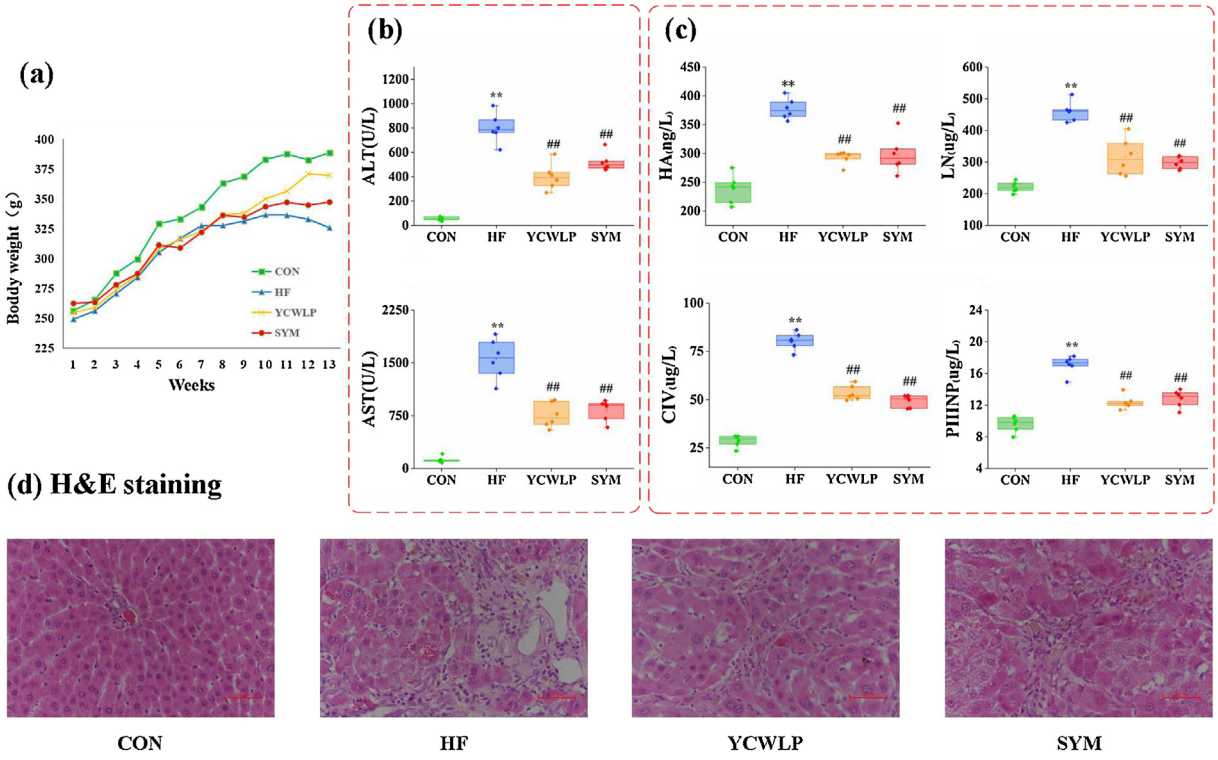

Fig. 1. Assessment of hepatic fibrosis in rats. (a) The changes of body weight during the experimental course (n = 6); (b) Serum ALT and AST after 8 weeks of YCWLP or SYM treatment (n = 6); (c) Serum HA, LN, CIV and PIIINP after 8 weeks of YCWLP or SYM treatment (n = 6); (d) Histopathological changes in rat livers among the CON, HF, YCWLP and SYM groups, stained with H&E (400×). ** represented significantly different with the CON group (p-value<0.01); ## represented significantly different with the HF group (p-value<0.01).

pathways involved. Metabolic pathways with p-value < 0.05 and impact-value > 0.10 were considered as potential pathways.

2.10. Statistical analysis

Data were analyzed by one-way ANOVA with Bonferroni's multiple comparisons test and Student's t-test using SPSS 19.0 (Chicago, IL, USA). p-value <0.05 was considered statistically significant.

3. Result

3.1. Assessment of hepatic fibrosis

In the whole process of the experiment, the weight growth trends of hepatic fibrosis groups were significantly slower than that of the CON group, which indicated that the establishment of the hepatic fibrosis model might be successful. The body weights of HF, YCWLP and SYM groups were similar in the first nine weeks. From the 10th week, the body weight of the HF group was gradually decreased, while the YCWLP group and SYM group were gradually showed an upward trend similar to the CON group (Fig. 1a).

The result of H&E staining showed that the morphology and structure of hepatic lobules in the CON group were complete, and the cytoplasm of hepatocytes was homogeneous without degeneration and necrosis. While for the HF group, the structure of hepatic lobule was destroyed, and there was obvious inflammatory infiltration, vacuole-like lesions, hepatic degeneration, necrosis and extensive hepatic fibrosis. Compared with the HF group, the vacuole-like lesions and necrosis of hepatocytes in the YCWLP group and SYM group were ameliorated, the cytoplasm was uniform, and the fibrotic grade was significantly lower (Fig. 1d).

The levels of ALT and AST in serum increased significantly in rats treated with CCl_4 compared with that of the CON group. YCWLP and SYM treatment reversed the CCl_4-induced changes in levels of ALT and AST in serum significantly (Fig. 1b). HA, LN, CIV and PIIINP are considered to be the most convenient and reliable indicators to reflect the degree of hepatic fibrosis. The results showed that the serum HA, LN, CIV and PIIINP levels were significantly increased in the HF group compared to the CON group, and the YCWLP and SYM treatment could significantly reverse all these four hepatic fibrosis indexes in serum (Fig. 1c). The results above indicate that YCWLP can protect hepatocytes and has a certain therapeutic effect on CCl_4-induced hepatic fibrosis.

3.2. Representative ^{1}H NMR spectra and total ions chromatographs (TICs)

Typical ^{1}H NMR spectra of the plasma, urine and liver samples at the 13th week are shown in Fig. S1, and the detailed metabolite assignments are listed in Table S3. A total of 41 plasma metabolites, 46 urine metabolites and 37 liver metabolites were assigned based on the ^{1}H NMR spectra. Representative TICs of the plasma, urine and liver samples at the 13th week were overlaid and shown in Fig. S1, and the differences were easily observed.

3.3. Metabolic trajectory analysis

The metabolic trajectories of plasma and urine samples among the CON, HF and YCWLP groups were analyzed at four time points (7th week, 9th week, 11th week and 13th week) (Fig. 2). The trace of metabolites clearly showed the time-dependent changes in different stages of treatment, and the arrow indicated the changing trend of metabolic profile. Plasma and urine metabolic trajectories of ^{1}H NMR and UPLC-MS showed that the CON group and HF group were completely separated from the 7th week. The metabolic profiles of the YCWLP group and HF group were basically overlapped at week 7, and showing a trend of separation from week 9, except for the NMR metabolic trajectories of urine, in which the YCWLP

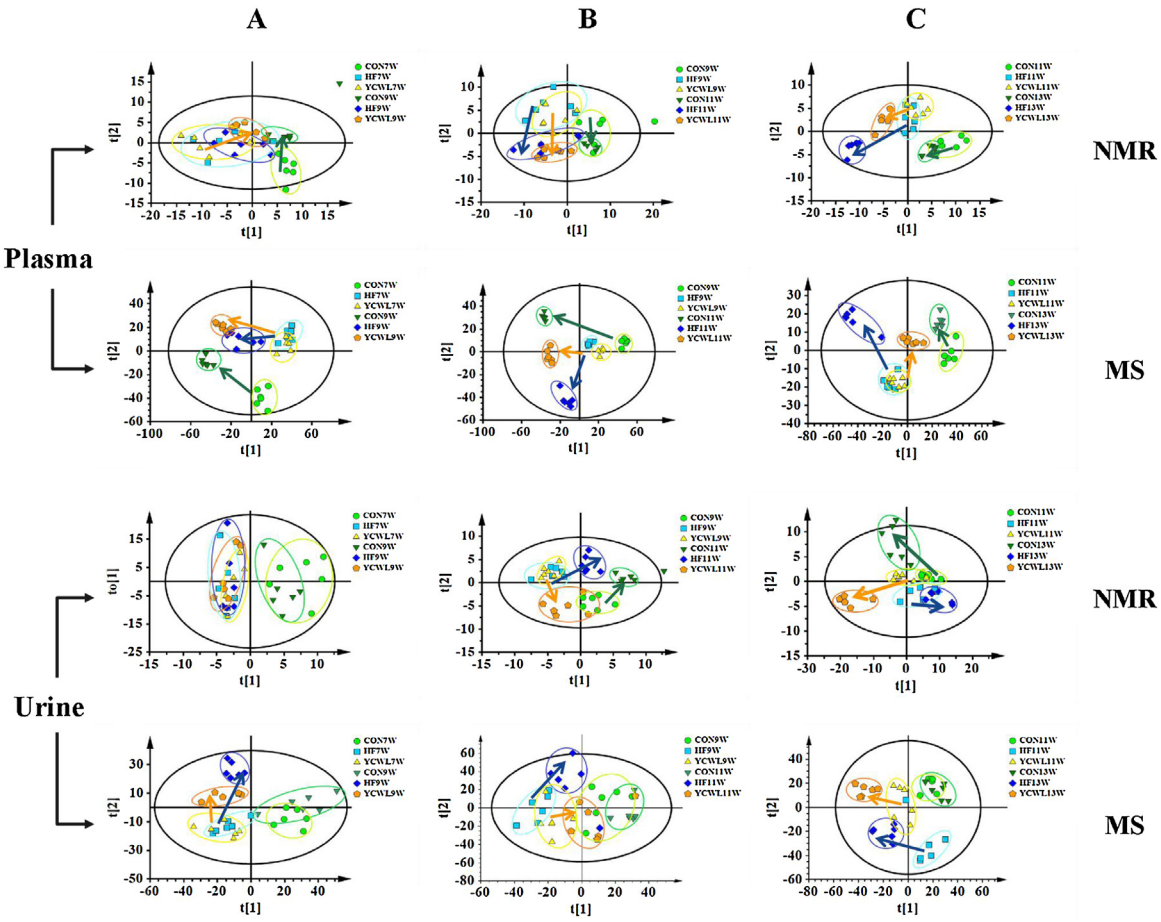

Fig. 2. The metabolic trajectory analysis of the plasma and urine samples among the CON, HF and YCWLP groups based on the OPLS-DA score plots. A, B, C denote: metabolic trajectories from week 7 to week 9 (A), metabolic trajectories from week 9 to week 11 (B), metabolic trajectories from week 11 to week 13 (C). The green arrow represents the CON group, the blue arrow represents the HF group, and the orange arrow represents the YCWLP group (For interpretation of the references to colour in this figure legend, the reader is referred to the web version of this article.).

group and HF group showed a trend of separation from week 11. With the extension of treatment time, the degree of separation gradually increased, and they were completely separated at the 11th week, except for the NMR metabolic trajectories of plasma, in which the YCWLP group and HF group were totally separated at week 13. In summary, the metabolic profiles of plasma and urine in the YCWLP group reached the maximum separation from that in the HF group at week 13, which suggested that YCWLP could adjust the changes of the metabolic profile in hepatic fibrosis rats. Therefore, the plasma, urine and liver samples of the 13th week were selected for multivariate data analysis and potential biomarker screening.

3.4. Metabolic profiling comparison between the CON and HF groups

The PCA score plots (Fig. 3A, C) of both ^{1}H NMR and UPLC-MS showed clear differences between the CON group and the HF group in plasma, urine and liver samples, which indicated that the establishment of the hepatic fibrosis model was successful. Meanwhile, the YCWLP group and the SYM group both showed a tendency to be far away from the HF group, and showed a trend close to the CON group except for the liver NMR plot, indicating that YCWLP and SYM intervention induced metabolic profile changes in the hepatic fibrosis rats. However, except for the plasma MS plot, the metabolic profiles of the YCWLP group and SYM group moved in different directions after treatment, which indicated that the mechanism of YCWLP reversing metabolic abnormalities caused by hepatic fibrosis was not consistent with SYM.

OPLS-DA was performed to disclose the metabolic differences among groups. The score plots (Fig. S2A, Fig. S3A) showed that the HF group was clearly separated from the CON group, and Fig. 3B and D showed the HF and YCWLP groups were obviously separated. Loading plots were further used to expose the candidate biomarkers (Fig.S2C, Fig.S3C, Fig.S4B, Fig.S4D). Endogenous metabolites with VIP > 1.2 and p-value < 0.05 were the candidate metabolites with significant changes.

As the results, 24 candidate metabolites in the plasma samples, 47 in the urine samples, and 24 in the liver samples significantly altered between the CON group and the HF group were identified (Table S4). There were 17 candidate metabolites in the plasma samples, 40 in the urine samples, and 10 in the liver samples significantly altered between the HF group and the YCWLP group (Table S5). Besides, the parameters of 7-fold cross-validation (Table S6) and permutations tests of PLS-DA (Fig. S2B, Fig. S3B, Fig. S4A, Fig. S4C) demonstrated that the models could exert well explanation and prediction.

3.5. Effect of YCWLP intervention on the metabolic profiles

The metabolites with statistically significant changes both between the CON group and the HF group and between the HF group and the YCWLP group were regarded as key metabolites of YCWLP affecting hepatic fibrosis. A total of 47 key metabolites identified were known to be regulated by YCWLP, including 9 plasma metabolites, 32 urine metabolites and 6 liver metabolites. Their specific information is shown in Table 1. The heatmap was also used

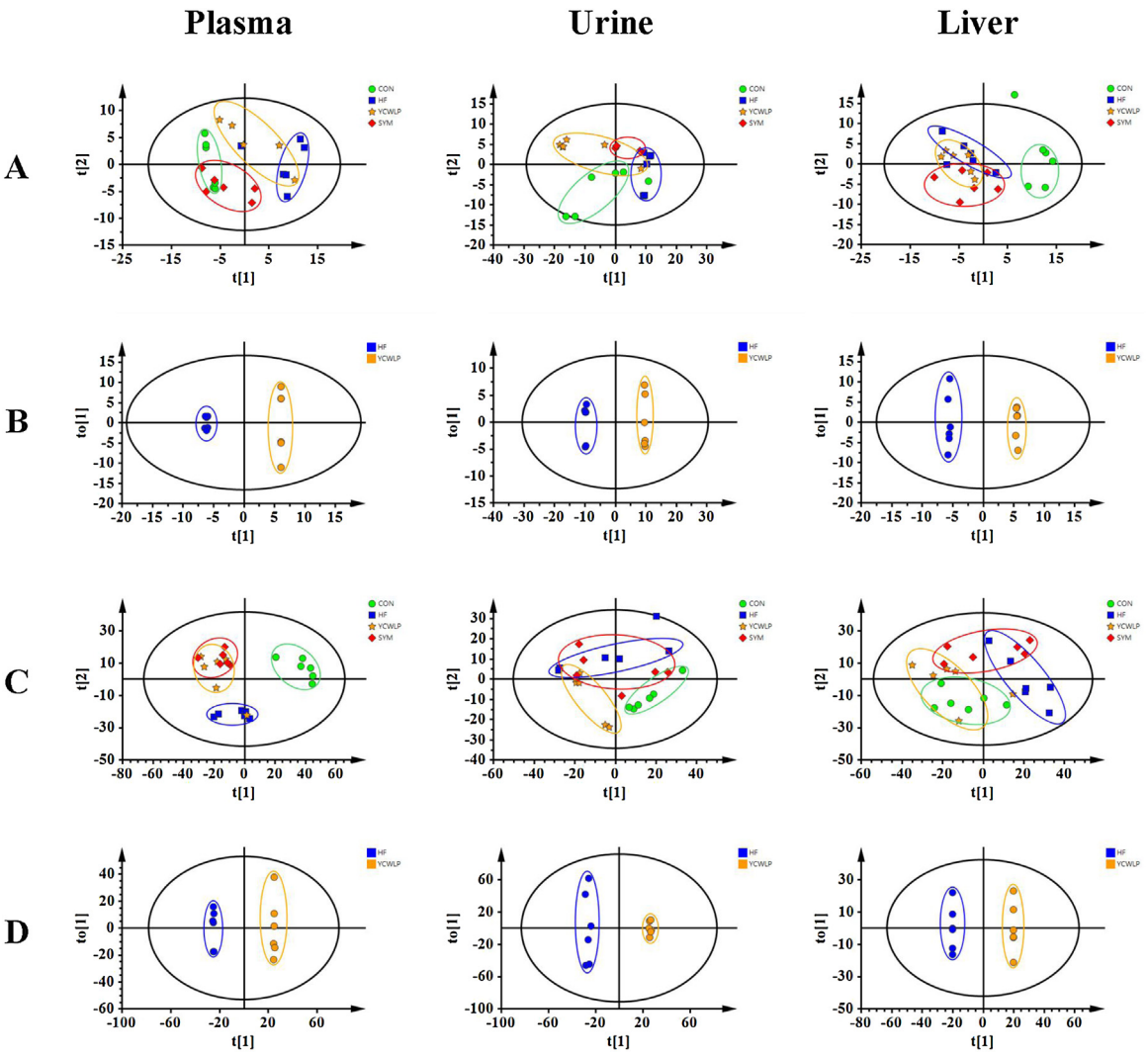

Fig. 3. Multivariate data analysis of the plasma, urine and liver samples. (A) PCA score plots of the CON, HF, YCWLP and SYM groups based on ^{1}H NMR spectra; (B) OPLS-DA score plots of the HF and YCWLP groups based on ^{1}H NMR spectra; (C) PCA score plots of the CON, HF, YCWLP and SYM groups based on UPLC-MS spectra; (D) OPLS-DA score plots of the HF and YCWLP groups based on UPLC-MS spectra.

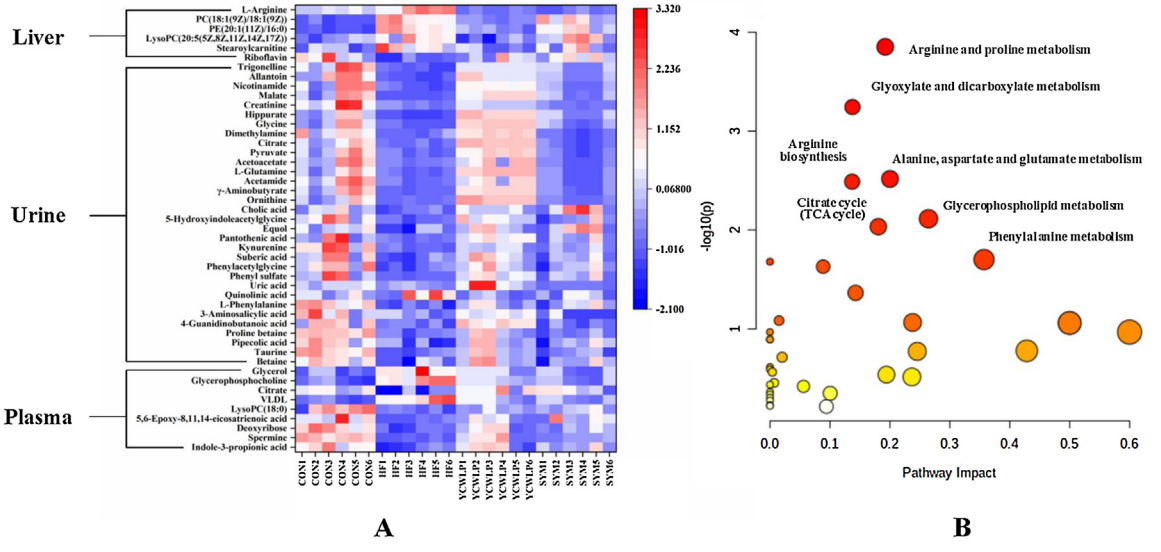

Fig. 4. **(A)** Heatmap of the key metabolites of hepatic fibrosis affected by YCWLP. Red indicates up-regulated metabolites and blue indicates down-regulated metabolites. **(B)** Meaningful pathways analysis based on potential biomarkers (p-value < 0.05, impact-value > 0.1). Bubble size is proportional to the impact of each pathway, and bubble color denotes the significance from the highest in red to the lowest in white (For interpretation of the references to colour in this figure legend, the reader is referred to the web version of this article.).

Table 1
Summary of the key metabolites of hepatic fibrosis affected by YCWLP in the plasma, urine and liver samples.

Biological matrices	Detect	Metabolites	Retention time(min) /Chemical shift (ppm)	Measured mass (m/z)	Fold change (Trend)		Biological matrices	Detect	Metabolites	Retention time(min) /Chemical shift (ppm)	Measured mass (m/z)	Fold change (Trend)	
					HF/CON	YCWLP/HF						HF/CON	YCWLP/HF
Plasma	*MS*	*Indole-3-propionic acid*	*1.82*	*190.45*	*0.31 (↓**)*	*2.45 (↑#)*	Urine	MS	5-Hydroxyindole-acetylglycine	5.46	248.91	0.33 (↓**)	2.60 (↑##)
	MS	Spermine	1.87	203.09	0.18 (↓**)	4.18 (↑#)		MS	Cholic acid	13.23	409.37	2.56 (↑*)	2.61 (↑##)
	MS	*Deoxyribose*	*1.82*	*269.65*	*0.26 (↓**)*	*2.32 (↑#)*		NMR	Ornithine	1.84 (m)	—	0.11 (↓**)	18.36 (↑##)
	MS	5,6-Epoxy-8,11,14-eicosatrienoic acid	9.49	343.13	0.32 (↓**)	1.86 (↑#)		NMR	γ-Aminobutyrate	**2.00 (m)**, 2.35 (t)	—	0.20 (↓**)	5.94 (↑##)
	MS	LysoPC (18:0)	17.62	546.36	0.34 (↓**)	1.59 (↑#)		NMR	Acetamide	2.04 (s)	—	0.28 (↓**)	3.04 (↑##)
	NMR	VLDL	0.89 (bs)	—	2.98 (↑**)	0.60 (↓#)		NMR	L-Glutamine	**2.14 (m)**, 4.31 (m)	—	0.25 (↓**)	5.52 (↑##)
	NMR	Citrate	2.57 (d), **2.70 (d)**	—	0.60 (↓**)	1.78 (↑##)		NMR	Acetoacetate	2.22 (s)	—	0.32 (↓*)	3.08 (↑##)
	NMR	Glycerophos-phocholine	3.23 (s)	—	2.21 (↑**)	0.68 (↓##)		NMR	Pyruvate	2.37 (s)	—	0.25 (↓**)	4.93 (↑##)
	NMR	Glycerol	**3.68 (m)**, 3.8 (m)	—	1.70 (↑**)	0.74 (↓#)		NMR	Citrate	**2.53 (d)**, 2.68 (d)	—	0.17 (↓**)	9.18 (↑##)
	MS	*Betaine*	*8.86*	*118.10*	*0.44 (↓**)*	*2.05 (↑#)*		NMR	Dimethylamine	2.72 (s)	—	0.37 (↓**)	3.15 (↑##)
	MS	Taurine	2.70	126.08	0.31 (↓**)	2.61 (↑##)		NMR	Glycine	3.57 (s)	—	0.38 (↓*)	3.67 (↑##)
	MS	*Pipecolic acid*	*10.84*	*130.07*	*0.42 (↓**)*	*1.92 (↑#)*		NMR	Hippurate	**4 (d)**, 7.56 (t), 7.64 (t)	—	0.29 (↓**)	5.24 (↑##)
	MS	Proline betaine	2.02	144.10	0.36 (↓**)	1.85 (↑#)		NMR	Creatinine	4.05 (s)	—	0.23 (↓**)	2.40 (↑##)
	MS	4-Guanidinobutanoic acid	2.13	146.10	0.37 (↓**)	3.05 (↑##)		NMR	Malate	4.31 (dd)	—	0.23 (↓**)	4.99 (↑##)
	MS	3-Aminosalicylic acid	3.79	153.95	0.43 (↓*)	1.88 (↑##)		NMR	Nicotinamide	4.44 (s)	—	0.19 (↓**)	4.95 (↑##)
Urine	MS	L-Phenylalanine	2.69	166.25	0.68 (↓*)	1.54 (↑#)		NMR	Allantoin	5.4 (s)	—	0.27 (↓**)	3.38 (↑##)
	MS	*Quinolinic acid*	2.70	168.24	0.44 (↓**)	1.58 (↑#)		NMR	Trigonelline	**8.84 (m)**, 9.13 (s)	—	0.21 (↓**)	3.43 (↑##)
	MS	Uric acid	2.28	168.97	0.60 (↓*)	3.01 (↑#)		MS	Riboflavin	7.02	377.18	0.36 (↓**)	2.19 (↑#)
	MS	Phenyl sulfate	8.60	174.89	0.26 (↓*)	3.59 (↑##)		MS	Stearoylcarnitine	13.15	428.45	1.60 (↑*)	0.60 (↓##)
	MS	Phenylacetylglycine	6.22	194.38	0.33 (↓**)	2.37 (↑##)	Liver	MS	LysoPC (20:5(5Z,8Z,11Z,14Z,17Z))	16.59	542.23	1.49 (↑*)	0.56 (↓##)
	MS	Suberic acid	11.59	197.17	0.28 (↓**)	3.26 (↑##)		MS	PE (20:1(11Z)/16:0)	17.03	746.72	4.99 (↑**)	0.42 (↓##)
	MS	Kynurenine	7.51	209.41	0.16 (↓**)	3.14 (↑##)		MS	PC (18:1(9Z)/18:1(9Z))	16.99	786.62	5.16 (↑**)	0.39 (↓##)
	MS	Pantothenic acid	8.60	220.64	0.30 (↓*)	3.20 (↑##)		NMR	L-Arginine	1.73 (m)	—	1.51 (↑**)	0.40 (↓##)
	MS	*Equol*	*12.19*	*243.19*	*0.48 (↓*)*	*2.13 (↑#)*							

The peak area corresponding to the chemical shift value in bold was used to draw the heatmap. Italics indicate metabolites with AUC < 0.85, and other metabolites were used for metabolic pathway analysis. "↑" and "↓" means the metabolite is up-regulated and down-regulated. **p*-value < 0.05, ***p*-value < 0.01, significant differences compared with the CON group. #*p*-value< 0.05, ##*p*-value < 0.01, significant differences compared with the HF group.

to visualize the changes in the metabolites, which exhibited the upregulated and downregulated metabolites in the plasma, urine, and liver samples (Fig. 4A).

ROC curves were drawn to evaluate the identification ability of key metabolites obtained from the above analysis. ROC curves of key metabolites between the CON and HF groups and between the HF and YCWLP groups were drawn, the metabolites with AUC values both greater than 0.85 were recognized as potential biomarkers. As the result, except for indole-3-propionic acid and deoxyribose in plasma, betaine, pipecolic acid, quinolinic acid and equol in urine, a total of 41 metabolites (including 7 metabolites in the plasma samples, 28 metabolites in the urine samples and 6 metabolites in the liver samples) were identified as potential biomarkers of YCWLP affecting hepatic fibrosis (Fig. 5).

3.6. Metabolic pathway analysis

41 potential biomarkers were imported into the MetaboAnalyst 5.0 for pathway analysis. Pathways with a p-value < 0.05 and an impact-value > 0.1 were considered as potential pathways that YCWLP affecting hepatic fibrosis. Fig. 4B and Table S7 show that there were seven primary disturbed pathways in HF rats treated by YCWLP, involving: (1) arginine and proline metabolism, (2) glyoxylate and dicarboxylate metabolism, (3) arginine biosynthesis, (4) alanine, aspartate and glutamate metabolism, (5) glycerophospholipid metabolism, (6) citrate cycle (TCA cycle), (7) phenylalanine metabolism.

4. Discussion

In this study, the protection of YCWLP on CCl_4-induced hepatic fibrosis was characterized by ^{1}H NMR and MS-based metabolomics analysis along with body weight change, serum liver function indexes, serum liver fibrosis index and histopathological observations of liver. The results showed that YCWLP could effectively increase the body weight and reduce the serum ALT, AST, HA, LN, CIV and PIIINP of rats with hepatic fibrosis. The histopathological analysis also showed that YCWLP could protect hepatocytes and reduce the degree of hepatic fibrosis. By analyzing the significant changes of metabolites among the CON group, HF group and YCWLP group, we found that YCWLP can significantly correct the disorder of seven metabolic pathways. A schematic diagram was drawn to show the relationship between potential biomarkers and metabolic pathways (Fig. 6).

4.1. Amino acid metabolism

YCWLP can affect four amino acid metabolic pathways, including: arginine and proline metabolism; arginine biosynthesis; alanine, aspartate and glutamate metabolism; phenylalanine metabolism.

Arginine is one of the key compounds in the urea cycle and the precursor of urea and nitric oxide (NO) [28]. When the liver is injured, the content of arginine increases, accompanied by the weakening of the urea cycle, leading to the accumulation of ammonia [29]. Clinical studies have shown that hyperammonemia and reduction of urea production are characteristic phenomena in patients with liver cirrhosis [30]. Ornithine is a basic amino acid produced by the catalytic decomposition of arginine by arginase, and urea is also produced in this process. In addition, arginine can also produce citrulline and release NO under the action of nitric oxide synthase. The two reactions require the same raw materials, so arginase and nitric oxide synthase will compete for arginine. After CCl_4 treatment, the activity of arginase decreased, and it was due to the leakage of a large number of enzymes into the systemic circulation, the release of lysosomal enzymes and the decrease of the concentration of IL-4 and IL-13 [31]. The diminished arginase activity indicates that arginine metabolism turned to citrulline synthesis [32]. Therefore, compared with the CON group, the L-arginine level of the HF group was increased, while the ornithine and metabolites of its downstream pathway were decreased in this study. These results indicate that the urea cycle of CCl_4-induced hepatic fibrosis rats was weakened, the toxic ammonia was accumulated in a large amount, which will further damage the liver tissue.

Glutamine is produced by glutamate and ammonia under the catalysis of glutamine synthetase. It is the main way of ammonia transportation and storage, and is very important for the body to maintain nitrogen balance [33]. It has been reported that glutamine could inhibit CCl_4-induced hepatic fibrosis in mice and TGF-β1 mediated epithelial-mesenchymal transition in mouse hepatocytes [34]. Furthermore, glutamine and alanine are glycogenic amino acids, which can be converted into glucose to supply energy when carbohydrate is insufficient [35]. The dysfunction of glutamine synthetase in the damaged hepatocytes will leads to the accumulation of harmful ammonia in the blood, which can lead to hepatic encephalopathy. Clinical studies showed that the levels of glutamine and glutamate in patients with hepatic fibrosis were significantly reduced [17]. In this study, the level of glutamine in the HF group decreased significantly, which was consistent with the literature.

Phenylalanine is an essential amino acid for the human body. Most of it is oxidized to tyrosine by phenylalanine hydroxylase. Together with tyrosine, it synthesizes important neurotransmitters and hormones, and participates in glucose metabolism and fat metabolism. The liver is the main place of phenylalanine metabolism. When the liver is damaged, the enzymes needed for phenylalanine metabolism are destroyed, resulting in the imbalance of phenylalanine metabolism.

After the intervention of YCWLP, the level of L-arginine was significantly decreased, while the level of 4-aminobutyrate, spermine, ornithine, 4-guanidinobutanoic acid, L-glutamine, pyruvate, citrate, L-phenylalanine and hippurate were significantly increased (Fig. 6), which indicates that YCWLP can regulate the disorder of the above four amino acids metabolic pathways in rats with hepatic fibrosis. Combined with the above analysis, it can be inferred that the therapeutic effect of YCWLP on hepatic fibrosis is mainly reflected in promoting the urea cycle, reducing blood ammonia accumulation, and activating energy metabolism by regulating amino acid levels.

4.2. Carbohydrate metabolism

YCWLP can affect two carbohydrate metabolism pathways, including: tricarboxylic acid (TCA) cycle; glyoxylate and dicarboxylate metabolism.

The TCA cycle is not only an important pathway involved in carbohydrate metabolism, but also a hub for the metabolism of carbohydrates, fat and amino acids [36]. Pyruvate is the product of the second stage of glycolysis, which enters the mitochondrial membrane under aerobic conditions, and decarboxylates to form acetyl CoA under the action of the pyruvate dehydrogenase system, and then enters the TCA cycle. It has been reported that the biological function of mitochondria in the rats with CCl_4-induced liver injury is damaged, the membrane stability is reduced, the energy metabolism and oxidative phosphorylation are inhibited, leading to abnormal liver energy metabolism [37]. Therefore, the metabolism of pyruvate and TCA cycle will be disturbed in rats with hepatic fibrosis. In this study, in the HF group, the contents of citrate and malate, which are important intermediates of the TCA cycle, were decreased as well as pyruvate, suggesting that the TCA cycle was

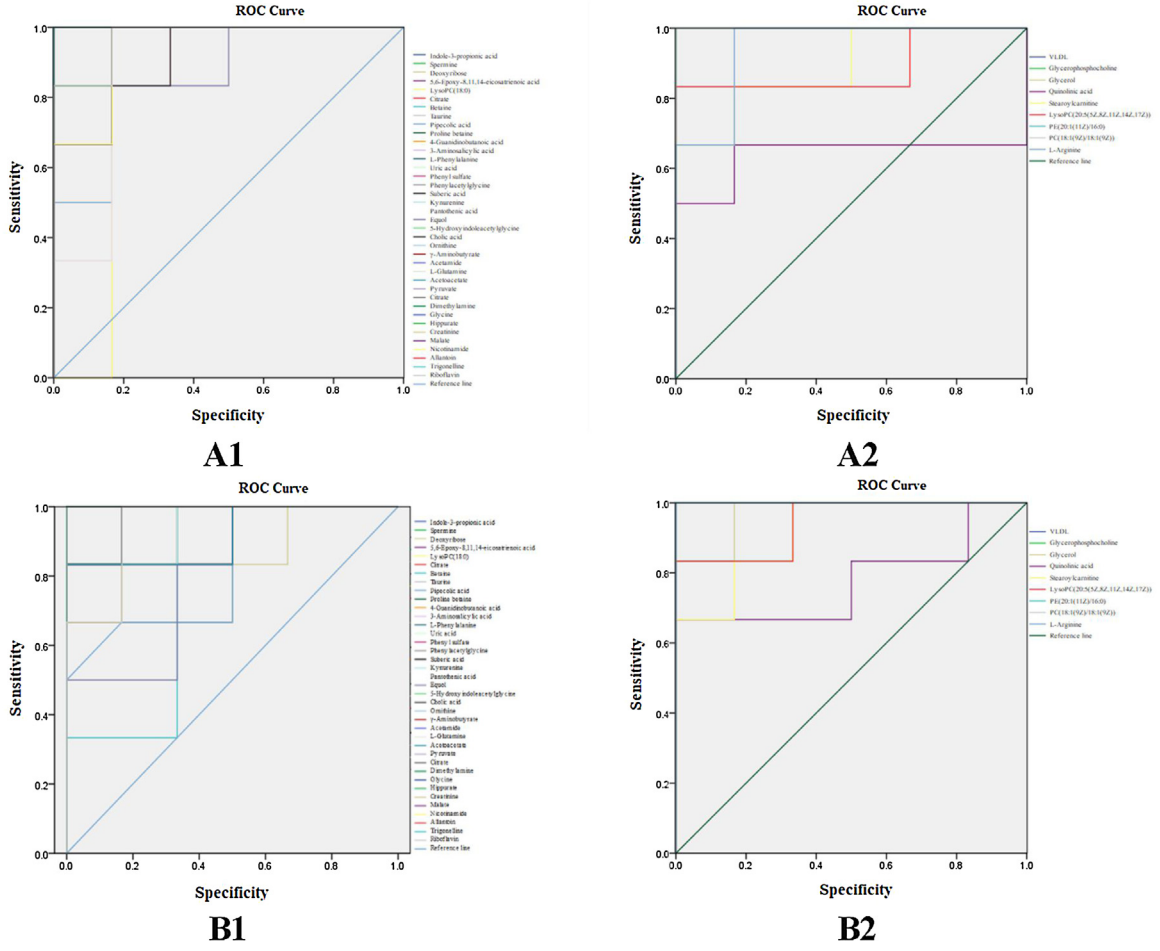

Fig. 5. Receiver operating characteristic (ROC) curves of the key metabolites. **(A1)** The down-regulated metabolites in the HF group compared with the CON group; **(A2)** The up-regulated metabolites in the HF group compared with the CON group; **(B1)** The up-regulated metabolites in the YCWLP group compared with the HF group; **(B2)** The down-regulated metabolites in the YCWLP group compared with the HF group.

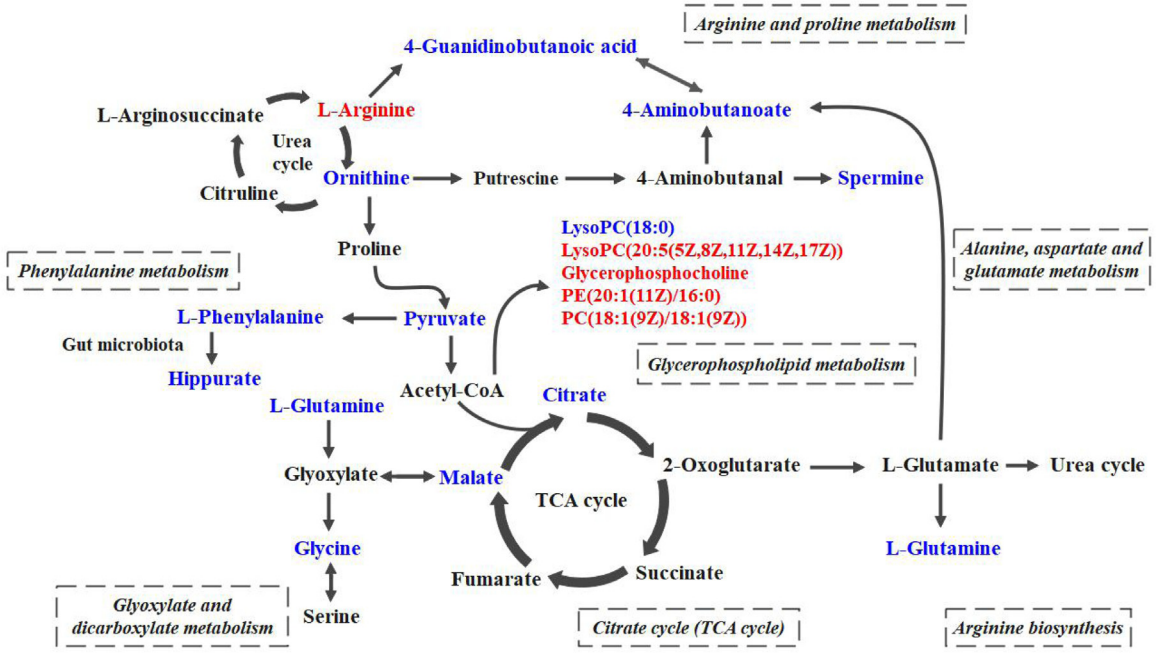

Fig. 6. The metabolic pathway networks resulting from YCWLP modulation to the CCl_4-induced hepatic fibrosis. Red indicates an increase in the metabolite in the HF group compared with the CON group and a decrease in the YCWLP group compared with the HF group. Blue indicates a decrease in the metabolite in the HF group compared with the CON group and an increase in the YCWLP group compared with the HF group. The changes mentioned above were statistically significant (p-value < 0.05) (For interpretation of the references to colour in this figure legend, the reader is referred to the web version of this article.).

down-regulated in the HF rats, and this may be related to mitochondrial dysfunction.

The metabolism of glyoxylate and dicarboxylate is related to the oxidation reaction in vivo, and the disturbance of this metabolism can indirectly lead to an abnormal TCA cycle [38]. Citrate, malate and pyruvate were involved in the metabolism of both glyoxylate and dicarboxylate and TCA cycle. The levels of these three substances decreased in the HF group, indicating that the carbohydrate metabolism was abnormal in the HF group after CCl_4 stimulation.

Glycine is synthesized by serine through the catalysis of related enzymes, which plays an important role in energy storage. Oxidative stress is the main pathogenesis of CCl_4-induced hepatic fibrosis in rats, and glycine is the precursor of the endogenous antioxidant glutathione. Therefore, in order to eliminate endogenous oxidants caused by CCl_4, the consumption of glutathione in liver is increased, and the pathway of glutathione synthesis by glycine is enhanced. This mechanism may be responsible for the decrease of glycine level in the HF group.

YCWLP intervention can significantly increase the levels of malate, citrate, pyruvate and glycine in urine and reverse the disorder of TCA intermediates (Fig. 6), which indicated that YCWLP can restore the disorder of carbohydrate metabolism, regulate the antioxidant capacity of hepatocytes and resist CCl_4 stress response.

4.3. Glycerophospholipid metabolism

Phosphoethanolamine (PE) and phosphocholine (PC) are key phospholipids of cell membrane [39], which are important intermediates involved in the synthesis of the characteristic bilayer structure of cells and regulate membrane integrity sensitivity to oxidative stress. Free radicals produced by CCl_4 can cause oxidative damage, resulting in the destruction of cell membrane structure, the disorder of choline and phospholipid metabolism, and the accumulation of PE and PC in rats with hepatic fibrosis [40]. Therefore, the contents of PE (20:1(11z)/16:0) and PC (18:1(9z)/18:1(9z)) in the HF group were significantly increased, which indicated an altered membrane phospholipids metabolism, and denoting the damage to the cell membrane.

Lysophosphatidylcholines (LysoPCs) are produced by phospholipase A2 (PLA2) hydrolyzing oxidized phosphatidylcholine in LDL, and play various roles in many biological processes. Compared with the CON group, the content of saturated LysoPCs (LysoPC (18:0)) in plasma of the HF group was significantly decreased, while the content of polyunsaturated LysoPCs (LysoPC(20:5(5Z,8Z,11Z,14Z,17Z))) in liver was significantly increased, which was consistent with previous research [41]. This trend is attributed to different mechanisms. Studies have shown that CCl_4 can increase the activity of PLA2 in the process of liver cancer modeling [42], resulting in an increase of LysoPCs content. On the other hand, LysoPCs can be produced by granulocytes through the release of reactive oxygen species (ROS), and the stimulation of CCl_4 can increase the oxidative damage of liver tissue, which also leads to the increase of LysoPCs level. However, hemolytic phospholipase D can increase the conversion of LysoPCs to lysophosphatidic acid, thus reducing the content of saturated LysoPCs in plasma [43]. This may explain the decrease of lysoPC (18:0) and the increase of lysoPC (20:5 (5Z, 8Z, 11z, 14z, 17Z)) in the HF group.

YCWLP can significantly inhibit the increase of PC (18:1(9z) /18:1(9z)), PE (20:1(11z)/16:0), LysoPC(20:5(5Z,8Z,11Z,14Z,17Z)), and the decrease of LysoPC (18:0) induced by hepatic fibrosis (Fig. 6), and regulate the disorder of glycerophospholipid metabolism, which may be one of the mechanisms of YCWLP in the treatment of hepatic fibrosis.

4.4. Gut bacteria metabolism

Studies have shown that the changes of microbial symbiotic metabolites in mammals often denotes the destruction of the structure of intestinal microbiota [44]. It has been reported that liver disease can cause changes in the intestinal flora, and the degree of intestinal flora imbalance is closely related to the progress of the liver disease [45]. Hippurate is formed by the combination of glycine and benzoic acid in liver tissue, and its level is related to the activity of intestinal flora [46]. In this study, the level of hippurate in the HF group was significantly lower than that in the CON group, indicating the disorder of intestinal flora in CCl_4-induced hepatic fibrosis rats. After YCWLP treatment, the level of hippurate increased significantly, which indicated that the therapeutic effect of YCWLP on hepatic fibrosis might be due to its regulation of the metabolism of intestinal flora.

5. Conclusion

In this study, ^{1}H NMR and MS-based metabolomics analysis along with body weight change, serum liver function indexes, serum liver fibrosis index and histopathological observations of liver were applied to evaluate the therapeutic effect of YCWLP on hepatic fibrosis and the mechanism associated with this. The results indicate that 7 metabolites in the plasma samples, 28 in the urine samples and 6 in the liver samples were identified as potential biomarkers of YCWLP affecting hepatic fibrosis, and these metabolites were primarily involved in amino acid metabolism, carbohydrate metabolism, glycerophospholipid metabolism and gut bacteria metabolism. By explaining the biological significance of these metabolic pathways, we found that YCWLP may treat CCl_4-induced hepatic fibrosis through the following four aspects: (1) promoting urea circulation and reducing blood ammonia accumulation; (2) improving carbohydrate metabolism and reducing oxidative stress; (3) improving glycerophospholipid metabolism and protecting cell membrane; (4) regulating intestinal flora metabolism. This study provides new insights into the hepatoprotective mechanism of YCWLP and lays a foundation for the further development of YCWLP as a potential therapeutic strategy for hepatic fibrosis.

CRediT authorship contribution statement

Yumeng Zhang: Conceptualization, Methodology, Visualization, Writing - original draft. **Min Zhao:** Methodology, Data curation, Writing - review & editing. **Yangyang Liu:** Investigation, Software, Validation. **Tingting Liu:** Validation, Writing - review & editing. **Chunjie Zhao:** Project administration, Supervision, Funding acquisition, Resources. **Miao Wang:** Funding acquisition, Project administration.

Declaration of Competing Interest

The authors report no declarations of interest.

Acknowledgments

This work was supported by the National Natural Science Foundation of China (NSFC: 81973284).

Appendix A. Supplementary data

Supplementary material related to this article can be found, in the online version, at doi:https://doi.org/10.1016/j.jpba.2021.114073.

References

[1] I. Okazaki, T. Wstanabe, S. Hozawa, M. Niioka, M. Arai, K. Maruyama, Reversibility of hepatic fibrosis:from the first report of collagenase in the liver to the possibility of gene therapy for recovery, Keio J. Med. 50 (2) (2001) 58–65.

[2] Z.Y. Zhang, W.B. Wang, L. Jin, X. Cao, G.H. Jian, N. Wu, X. Xu, Y. Yao, D.S. Wang, iTRAQ-based quantitative proteomics analysis of the protective effect of yinchenwuling powder on hyperlipidemic rats, Evid.-Based Compl. Alt. 2017 (2017), 3275096.

[3] D.Y. Wang, Efficacy observation of Yin chen Wu Ling Powder with ingredients added or subtracted in the treatment of 126 cases of neonatal hyperbilirubinemia, J. Pediatrics Tradit. Chin. Med. 7 (06) (2011) 25–26.

[4] Q. Ma, The therapeutic effect of Yinchen Wuling powder on children with acute jaundice hepatitis, Chin. Pediatr. Integr. Tradit. Western Med. 12 (03) (2020) 258–260.

[5] C.Z. Zhu, H. Li, Clinical observation of Yinchen Wuling powder in the treatment of 65 cases of refractory ascites due to liver cirrhosis, Nei Mongol J. Tradit. Chin. Med. 29 (09) (2010) 32.

[6] B. Chen, Clinical study of Yinchen Wuling powder on liver function and serum indexes in patients with liver fibrosis, Shandong J. Tradit. Chin. Med. 31 (03) (2012) 162–164.

[7] X.L. Liu, L.H. Zhao, 50 cases of nonalcoholic fatty liver treated with Yinchen Wuling powder, Shanxi J. Tradit. Chin. Med. 32 (05) (2011) 520–521.

[8] Y.Q. Bian, B.B. Ning, H.Y. Cao, Y. Lu, C. Liu, G.F. Chen, J. Liu, P. Liu, M.Y. Sun, Formula-syndrome correlation study of three classical anti-jaundice formulas in inhibition of liver fibrosis induced by dimethylnitrosamine in rats, J. Integr. Med. 10 (12) (2012) 1405–1412.

[9] Z.H. Xie, J. Qiang, X.B. Pi, Y.H. Chen, Q. Yu, Q. Zhang, Favorable outcome of adjunctive traditional Chinese medicine therapy in liver cirrhosis: a large cohort study in Southwest China, Complement. Ther. Med. 51 (2020), 102446.

[10] D.S. Wishart, Metabolomics for investigating physiological and pathophysiological processes, Physiol. Rev. 99 (4) (2019) 1819–1875.

[11] Y.Q. Wang, J.Y. Yan, B.M. Shi, S.X. Li, L. Wang, L. Wang, Research Progress on material basis of efficacy of Chinese herbal compound, Chin. J. Inf. Tradit. Chin. Med. 19 (05) (2012) 99–102.

[12] A. Elmsjo, J. Haglof, M.K.R. Engskog, M. Nestor, T. Arvidsson, C. Pettersson, The co-feature ratio, a novel method for the measurement of chromatographic and signal selectivity in LC-MS-based metabolomics, Anal. Chim. Acta 956 (2017) 40–47.

[13] J. Azmi, J. Connelly, E. Holmes, J.K. Nicholson, R.F. Shore, J.L. Griffin, Characterization of the biochemical effects of 1-nitronaphthalene in rats using global metabolic profiling by NMR spectroscopy and pattern recognition, Biomarkers 10 (6) (2005) 401–416.

[14] M.P.M. Letertre, G. Dervilly, P. Giraudeau, Combined nuclear magnetic resonance spectroscopy and mass spectrometry approaches for metabolomics, Anal. Chem. 93 (1) (2021) 500–518.

[15] D.D. Marshall, R. Powers, Beyond the paradigm: combining mass spectrometry and nuclear magnetic resonance for metabolomics, Prog. Nucl Mag. Res. Sp. 100 (2017) 1–16.

[16] Z.Y. Li, Y. Li, L.P. Lu, Z.H. Yang, W.H. Xue, X. Tian, X.J. Zhang, ^{1}H-NMR based serum metabolomics study to investigate hepatoprotective effect of Qin-Jiao on carbon tetrachloride-induced acute hepatotoxicity in rats, Evid.-Based Compl. Alt. 2017 (2017), 6091589.

[17] N. Embade, Z. Mariño, T. Diercks, A. Cano, S. Lens, D. Cabrera, M. Navasa, J.M. Falcon-Perez, J. Caballeria, A. Castro, J. Bosch, J.M. Mato, O. Millet, Metabolic characterization of advanced liver fibrosis in HCV patients as studied by serum ^{1}H-NMR spectroscopy, PLoS One 11 (5) (2016), e0155094.

[18] L. An, Q.L. Lang, W.B. Shen, Q.S. Shi, F. Feng, Dynamic metabolic profiling of urine biomarkers in rats with alcohol-induced liver damage following treatment with Zhi-Zi-Da-Huang decoction, Mol. Med. Rep. 14 (3) (2016) 2093–2100.

[19] M.J.W. McPhail, S. Montagnese, M. Villanova, H. El Hadi, P. Amodio, M.M.E. Crossey, R. Williams, I.J. Cox, Urinary metabolic profiling by ^{1}H NMR spectroscopy in patients with cirrhosis may discriminate overt but not covert hepatic encephalopathy, Metab. Brain Dis. 32 (2) (2017) 331–341.

[20] D.D. Wei, J.S. Wang, M.H. Li, P.P. Guo, G. Dong, M.H. Yang, L.Y. Kong, A pilot study of the onset of hepatic encephalopathy (OHE) in mice induced by thioacetamide and the protective effect of taurine by holistic metabolic characterization, Metabolomics 11 (3) (2015) 559–570.

[21] D.S. Zhao, Z.T. Wu, Z.Q. Li, L.L. Wang, L.L. Jiang, W. Shi, P. Li, H.J. Li, Liver-specific metabolomics characterizes the hepatotoxicity of Dioscorea bulbifera rhizome in rats by integration of GC-MS and ^{1}H-NMR, J. Ethnopharmacol. 226 (2018) 111–119.

[22] Y.Q. Song, T.T. Hu, H. Gao, J.H. Zhai, J.W. Gong, Y.M. Zhang, L.N. Tao, J.M. Sun, Z.Y. Li, X.Y. Qu, Altered metabolic profiles and biomarkers associated with astragaloside IV-mediated protection against cisplatin-induced acute kidney injury in rats: an HPLC-TOF/MS-based untargeted metabolomics study, Biochem. Pharmacol. 183 (2021), 114299.

[23] Y.H. Jiang, P. Zhang, Y.N. Tao, Y. Liu, G.S. Cao, L. Zhou, C.H. Yang, Banxia Baizhu Tianma decoction attenuates obesity-related hypertension, J. Ethnopharmacol. 266 (2021), 113453.

[24] H.J. Li, W.L. Cao, M.X. Lu, C.X. Wu, X.G. Wang, L.Y. Niu, Urinary and serum metabolomics analyses uncover that total glucosides of paeony protect liver against acute injury potentially via reprogramming of multiple metabolic pathways, Evid.-Based Compl. Alt. 2017 (2017), 9038260.

[25] S. Chen, M.Y. Zhang, L. Bo, S.Q. Li, L.Y. Hu, X.J. Zhao, C.H. Sun, Metabolomic analysis of the toxic effect of chronic exposure of cadmium on rat urine, Environ. Sci. Pollut. R. 25 (4) (2018) 3765–3774.

[26] R.H. Chen, Q. Wang, L.J. Zhao, S.L. Yang, Z.F. Li, Y.L. Feng, J.Q. Chen, C.N. Ong, H. Zhang, Lomatogonium rotatum for treatment of acute liver injury in mice: a metabolomics study, Metabolites 9 (10) (2019) 227.

[27] Y. Yuan, X. Wu, Y.L. Hong, X. Zhang, Z.Y. Wang, H.Y. Yan, Salidroside ameliorates liver metabonomics in relation to modified gut-liver FXR signaling in furan-induced mice, Food Chem. Toxicol. 140 (2020), 111311.

[28] X.S. Ma, Y.C. Zhang, D. Jiang, Y. Yang, G.Y. Wu, Z.L. Wu, Protective effects of functional amino acids on apoptosis, inflammatory response, and pulmonary fibrosis in lipopolysaccharide-challenged mice, J. Agr. Food Chem. 67 (17) (2019) 4915–4922.

[29] K.J. Dabos, J.A. Parkinson, I.H. Sadler, J.N. Plevris, P.C. Hayes, ^{1}H nuclear magnetic resonance spectroscopy-based metabonomic study in patients with cirrhosis and hepatic encephalopathy, World J. Hepatol. 7 (12) (2015) 1701–1707.

[30] K. Weissenborn, B. Ahl, D. Fischer-Wasels, J. van den Hoff, H. Hecker, W. Burchert, H. Kostler, Correlations between magnetic resonance spectroscopy alterations and cerebral ammonia and glucose metabolism in cirrhotic patients with and without hepatic encephalopathy, Gut 56 (12) (2007) 1736–1742.

[31] S. Vijaya, B. Nagarajan, Arginine metabolism in rat liver after hepatic damage, Biochem. Med. (Zagreb) 27 (1) (1982) 86–94.

[32] D. Popović, G. Kocić, V. Katić, A. Zarubica, L.J. Velickovic, V.P. Nickovic, A. Jovic, A. Veljkovic, V. Petrovic, V. Rakic, Z. Jovic, N.P. Ulrih, D. Sokolovic, M. Stojanovic, M. Stankovic, G. Radenkovic, G.R. Nikolic, A. Lukac, A. Milosavljevic, D. Sokolovic, Anthocyanins protect hepatocytes against CCl_4-Induced acute liver injury in rats by inhibiting pro-inflammatory mediators, polyamine catabolism, Lipocalin-2, and excessive proliferation of kupffer cells, Antioxidants 8 (10) (2019) 451.

[33] I.D. Weiner, J.W. Verlander, Ammonia transporters and their role in acid-base balance, Physiol. Rev. 97 (2) (2017) 465–494.

[34] N. Shrestha, L. Chand, M.K. Han, S.O. Lee, C.Y. Kim, Y.J. Jeong, Glutamine inhibits CCl4 induced liver fibrosis in mice and TGF-β1 mediated epithelial-mesenchymal transition in mouse hepatocytes, Food Chem. Toxicol. 93 (2016) 129–137.

[35] G. Fan, Q. Li, H.J. Li, Y.S. Zhang, X.M. Xu, G. Fan, Y.M. Ge, L.L. Du, Active ingredients and anti-arthritic mechanisms of Ba-Wei-Long-Zuan granule revealed by ^{1}H-NMR-Based metabolomics combined with network pharmacology analysis, Chem. Biodivers. 17 (2020), e2000122.

[36] Y.R. Liu, R.Q. Huang, L.J. Liu, J.N. Peng, B.K. Xiao, J.Y. Yang, Z.C. Miao, H.L. Huang, Metabonomics study of urine from Sprague-Dawley rats exposed to Huang-yao-zi using ^{1}H NMR spectroscopy, J. Pharm. Biomed. Anal. 52 (1) (2010) 136–141.

[37] L.R. Zhang, S.Q. Wang, H.Y. Wang, R.Y. Dong, S.N. Meng, Effect of mitochondrial dysfunction introduced by chronic liver injury in rats, J. Chin, Med. Univ. 49 (8) (2020) 747–751.

[38] X.J. Liu, C.C. Liu, J.S. Tian, X.X. Gao, K. Li, G.H. Du, X.M. Qin, Plasma metabolomics of depressed patients and treatment with Xiaoyaosan based on mass spectrometry technique, J. Ethnopharmacol. 246 (2020), 112219.

[39] G.V. Meer, D.R. Voelker, G.W. Feigenson, Membrane lipids: where they are and how they behave, Nat. Rev. Mol. Cell Biol. 9 (2) (2008) 112–124.

[40] L.W.D. Weber, M. Boll, A. Stampfl, Hepatotoxicity and mechanism of action of haloalkanes: carbon tetrachloride as a toxicological model, Crit. Rev. Toxicol. 33 (2) (2003) 105–136.

[41] S.F. Li, H.X. Liu, Y.B. Jin, S.H. Lin, Z.W. Cai, Y.Y. Jiang, Metabolomics study of alcohol-induced liver injury and hepatocellular carcinoma xenografts in mice, J. Chromatogr. B 879 (24) (2011) 2369–2375.

[42] R. Angelini, G. Vortmeier, A. Corcelli, B. Fuchs, A fast method for the determination of the PC/LPC ratio in intact serum by MALDI-TOF MS: an easy-to-follow lipid biomarker of inflammation, Chem. Phys. Lipids 183 (2014) 169–175.

[43] N. Watanabe, H. Ikeda, K. Nakamura, R. Ohkawa, Y. Kume, T. Tomiya, K. Tejima, T. Nishikawa, M. Arai, M. Yanase, J. Aoki, H. Arai, M. Omata, K. Fujiwara, Y. Yatomi, Plasma lysophosphatidic acid level and serum autotaxin activity are increased in liver injury in rats in relation to its severity, Life Sci. 81 (12) (2007) 1009–1015.

[44] F.P.J. Martin, M.E. Dumas, Y.L. Wang, C. Legido-Quigley, I.K.S. Yap, H.R. Tang, S. Zirah, G.M. Murphy, O. Cloarec, J.C. Lindon, N. Sprenger, L.B. Fay, S. Kochhar, P. van Bladeren, E. Holmes, J.K. Nicholson, A top-down systems biology view of microbiome-mammalian metabolic interactions in a mouse model, Mol. Syst. Biol. 3 (2007) 122.

[45] I. Gómez-Hurtado, A. Santacruz, G. Peiró, P. Zapater, A. Gutierrez, M. Perez-Mateo, Y. Sanz, R. Frances, Gut microbiota dysbiosis is associated with in flammation and bacterial translocation in mice with CCl_4-induced fibrosis, PLoS One 6 (7) (2011), e23037.

[46] Q.Y. Niu, Z.Y. Li, G.H. Du, X.M. Qin, ^{1}H NMR based metabolomic profiling revealed doxorubicin-induced systematic alterations in a rat model, J. Pharm. Biomed. Anal. 118 (2016) 338–348.